Available online at www.sciencedirect.com
SCIENCE DIRECT®
Biochemical and Biophysical Research Communications 319 (2004) 636–642
BBRC
www.elsevier.com/locate/ybbrc

Binding site of *Escherichia coli* RNA polymerase to an RNA promoter

Martin Pelchat[a,*] and Jean-Pierre Perreault[b]

[a] *Department of Biochemistry, Microbiology and Immunology, Faculty of Medicine, University of Ottawa, 451 Smyth Road, Ottawa, Ont., Canada K1H 8M5*
[b] *Département de Biochimie, Faculté de Médecine, Université de Sherbrooke, 3001 12ème avenue, Sherbrooke, Que., Canada J1H 5N4*

Received 6 May 2004

Abstract

The DNA-dependent RNA polymerase (RNAP) from *Escherichia coli* has previously been reported to specifically initiate transcription from viroid-derived RNA promoters in vitro. In order to gain insight into the molecular mechanism of RNA promoter recognition by this RNAP, we have used nucleic acid intercalators and RNA:protein footprinting experiments to study the interaction between the polymerase and an RNA promoter at the initiation site. Our data revealed that the polymerase binds an external single-stranded loop, rather than a double-stranded region as is the case for DNA templates. Despite this divergence in promoter binding, the model RNA template was bound by both the β and β′ subunits of the RNAP, as is observed with DNA templates. Most importantly, this work proposes large single-stranded RNA hairpin loops have the potential to be promoters for DNA-dependent RNAP.

Keywords: RNA promoter; Viroid; RNA polymerase binding site; Transcription initiation; Rolling circle replication

Several DNA-dependent RNA polymerases (RNAP) have been shown to possess the ability to use RNA molecules as templates when a suitable one is offered [1]. Among the various natural RNA species that might take advantage of this property of DNA-dependent RNAPs for their replication, viroids are the simplest and the best characterized. Viroids are small (~300 nucleotides, nt), single-stranded, circular, non-coding RNA pathogens (for a review see [2]). They replicate by a rolling circle mechanism that follows either a symmetric or an asymmetric mode. In the symmetric mode the infecting circular monomer (which is assigned plus polarity by convention) is replicated into linear multimeric minus strands which are then cleaved and ligated, yielding minus circular monomers. Using the latter RNA as template, the same three steps are then repeated to produce the plus progeny. In contrast, in the asymmetric mode, the linear multimeric minus strands serve directly as the template for the synthesis of linear multimeric plus strands. Because they replicate exclusively via RNA intermediates, and rely entirely on their host's RNAP for this replication, viroids are therefore ideally suited for analyses of RNA amplification by DNA-dependent RNAP.

The DNA-dependent RNAP from *Escherichia coli* (*E. coli*) has been shown to specifically initiate the replication of peach latent mosaic viroid (PLMVd) in vitro using PLMVd-derived RNAs of both plus and minus polarities as templates [3]. Regardless of the polarity of the PLMVd strand used as template, the RNA feature that triggers the RNAP to initiate specific transcription was showed to be a hairpin structure (Fig. 1A) [4]. The characterization of this RNA promoter revealed that any structural alteration that disrupts the overall rod-like conformation of the template interferes with transcription. In addition, it was demonstrated that its specific sequence does not have to be conserved, as long as it possesses a base-paired uridine as the primary initiation site, and that this uridine must be the first nucleotide 5′ of a loop composed of at least 6 nt. The presence of a relatively unstable stem (i.e., one possessing a low percentage of GC base-pairing) adjacent to the initiation site was also shown to significantly increase the level of transcription.

* Corresponding author. Fax: +1-613-562-5452.
E-mail address: mpelchat@uottawa.ca (M. Pelchat).

0006-291X/$ - see front matter © 2004 Elsevier Inc. All rights reserved.
doi:10.1016/j.bbrc.2004.05.044

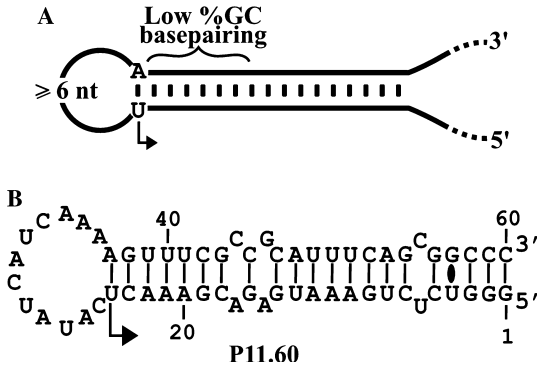

Fig. 1. Structure of the RNA promoter. (A) Schematic representation of the RNA promoter according to a previous report [4]. (B) Sequence and secondary structure of the P11.60 RNA template. The primary initiation site is indicated by an arrow.

The RNAP from *E. coli* is composed of a catalytic core (i.e., the $\alpha_2\beta\beta'$ subunits) and a σ^{70} subunit (for a review see [5]). The presence of both the catalytic core and the σ^{70} subunit has been shown to be essential for transcription from PLMVd-derived RNA promoters [4]. In contrast to what is reported with a DNA template, the σ^{70} subunit was shown to be responsible for neither the recognition of the RNA promoter sequence nor the melting of the helix at the initiation fork. However, it was suggested that upon binding to the core RNAP, the σ^{70} subunit might support a conformational change that permits initiation to occur [4].

The goal of the present work was to identify the site of binding of the *E. coli* RNAP to an RNA promoter. In order to gain insight into the molecular mechanism of RNA promoter recognition by a DNA-dependent RNAP, the interactions between the RNAP from *E. coli* and the P11.60 RNA promoter (Fig. 1B), as representative of enzyme and template, respectively, were studied.

Materials and methods

Transcription assays using E. coli RNAP. Transcription reactions were performed as described previously [4]. Briefly, 50 pmol of either P11.60 RNA template (synthesized by in vitro transcription in the presence of T7 RNA polymerase from a template composed of two complementary DNA oligonucleotides) or a DNA template (i.e., pBlueScript KS DNA digested by *Sca*I) was transcribed by the RNAP from *E. coli* (0.9 pmol; Amersham Biosciences) in 50 μL of transcription buffer (40 mM Tris–HCl, pH 8.0, 10 mM $MgCl_2$, 150 mM KCl, 5 mM dithiothreitol, and 5 μg/mL BSA) containing 0.2 mM NTP, 50 μCi [γ-^{32}P]ATP (3000 Ci/mmol; Amersham Biosciences), and different concentrations of intercalator agents. The reactions were incubated at 37 °C for 60 min, stopped by the addition of 25 μL of stop buffer (80% formamide, 10 mM EDTA, pH 8.0, 0.25% each of xylene cyanol, and bromophenol blue), and then fractionated through denaturing 5% or 20% PAGE gels for DNA and RNA templates, respectively. The intensity of the bands was determined by phosphorimager scanning.

Electrophoretic mobility-shift assays. Either a double-stranded σ^{70}-driven DNA template (5′-GCTAACTTGTTTTGACACCGGGTC TATTTGGTGGTATAATAGATTCATACATTTTTGCCT-3′, the underlined nucleotides correspond, in the order, to the −35 box, −10 box and the initiation site), or the P11.60 RNA template was end-labeled with [γ-^{32}P]ATP using T4 polynucleotide kinase according to the manufacturer's recommended protocol (New England Biolabs). Radiolabeled templates (1 pmol) were dissolved in a final volume of 10 μL of transcription buffer containing 0.9 pmol of *E. coli* RNAP and increasing amounts of ethidium bromide (0, 0.5, 1, 5, 10, 50, and 100 μM). After incubation at room temperature for 30 min, 3 μL of glycerol solution (30% glycerol, 0.25% xylene cyanol, and 0.25% bromophenol blue) was added and the resulting mixtures were electrophoresed through native 5% PAGE gels (49:1 ratio of acrylamide to bisacrylamide) in 1× TBE buffer (100 mM Tris–borate, pH 8.3, 1 mM EDTA) at room temperature and low voltage. The gels were then exposed to a phosphor screen.

RNase H hydrolysis. Trace amounts of internally labeled P11.60 RNA were preincubated either with or without the RNAP from *E. coli* (2 μM) for 30 min at 25 °C in a final volume of 18 μL of transcription buffer. Subsequently, DNA oligonucleotides (5′-GATGATATG-3′; 20 μM) and RNase H (0.5 U; United States Biochemicals) were added and the samples were incubated at 25 °C for 10 min. The reactions were quenched by adding 6 μL stop buffer, the mixtures were fractionated through a denaturing 10% PAGE gel as described above, and the gel was exposed to a phosphor screen.

UV crosslinking of the RNAP:P11.60 complex. To increase the crosslinking efficiency, the P11.60 RNA was synthesized in the presence of 4-thio-uridine triphosphate (TriLink BioTech) during the transcription and gel-purified. The resulting P11.60 RNA was labeled either at the 5′-end using T4 polynucleotide kinase in the presence [γ-^{32}P]ATP, or at the 3′-end using T4 RNA ligase and [α-^{32}P]pCp (Amersham BioSciences), and gel-purified. End-labeled P11.60 RNAs were incubated with the RNAP from *E. coli* as described above, and UV crosslinked by exposition for 10 min to 365 nm light using a UV crosslinker (Hoefer) at a distance of ~4 cm. The resulting mixtures were then diluted in 1 volume of SDS loading dye (50 mM Tris–HCl, pH 6.8, 2% SDS, 0.1% BPB, and 10% glycerol), the RNAP:P11.60 RNA complexes were fractionated on a 10% SDS–PAGE gel and detected by autoradiography.

Partial alkaline hydrolysis of the RNAP:P11.60 complexes. Following UV crosslinking the complexes were fractionated as above on a 10% SDS–PAGE gel, the appropriate bands were excised and electroeluted in Tris–glycine electrophoresis buffer (25 mM Tris–HCl, pH 8.3, 250 mM glycine, and 0.1% SDS). After precipitation, the RNAP:P11.60 template complexes were either reserved or partially hydrolyzed by incubating in 0.3 M NaOH for 2 min at 25 °C, the reactions stopped by adding 1 vol of 1 M Tris–HCl, pH 7.5, and ethanol precipitated. The resulting pellets were dissolved in stop buffer, fractionated through a 10% denaturing PAGE gel, and visualized by exposure to a phosphor screen.

Fluorescence measurements. Fluorescence emission spectra were conducted on an Hitachi F-2500 fluorescence spectrophotometer using an excitation wavelength of 335 nm on various combinations of the double-stranded σ^{70}-driven DNA template (0.2 μM), the P11.60 RNA promoter (0.2 μM), and the *E. coli* RNAP (0.2 μM) preincubated in transcription buffer. Ethidium bromide (1 μM) was then added and the emission spectra were collected from 550 to 650 nm. Background emission was eliminated by subtracting the signal from the buffer alone.

Results

Effect of intercalator agents on the transcription reaction

In order to investigate the effect of intercalator agents on the transcription reaction, we adopted an enzymatic assay that was described previously in great detail [4].

Briefly, either the P11.60 RNA promoter (see Fig. 1B), or a typical DNA promoter (i.e., a DNA fragment that includes both −10 and −35 boxes of a promoter obtained by *Sca*I digestion of the pBlueScript KS vector) was transcribed by the RNAP from *E. coli* in the presence of [γ-^{32}P]ATP and different intercalator agents. This radioactive nucleotide was used because it allows identification of only newly synthesized RNA molecules, since they are the only ones that contain a new 5′-terminal triphosphate group (pppN). The resulting mixtures were analyzed by denaturing polyacrylamide gel electrophoresis (PAGE), and the relative intensities of each band were determined (Fig. 2A inset). Actinomycin-D, Hoechst 33258, and ethidium bromide were found to strongly inhibit transcription from the DNA template (Figs. 2A–C; open squares). These results are in agreement with an earlier report using another DNA template [6]. Nucleic acid intercalators are characterized by a substantially higher affinity for double-stranded, as compared to single-stranded, nucleic acids [6–8]. By binding to double-strand nucleic acids, they inflate double-stranded nucleic acids, producing an alteration in the orientation of the helix. When acting on a DNA template, the RNAP initially forms contacts with the surface of the promoter helix [9]. Therefore, when added before the RNAP, the intercalation of these agents can prevent the binding of the enzyme to a double-stranded promoter and inhibit the transcription reaction [6]. In order to verify the effect of the intercalator agents with a RNA template, we used a hairpin structure with a loop composed of at least 6 nt that was shown to be the minimal features required to support the initiation of transcription [4]. The three intercalator agents also inhibited transcription from the P11.60 RNA template, although at a reduced level (Figs. 2A–C; closed circles). The inhibitory effect of these compounds was found to be more than one order of magnitude greater on DNA template than on the P11.60 RNA template. Concentrations of less than 0.3 μM of these agents caused greater than 50% inhibition of transcription from the DNA template, while concentrations of 24 ± 3, 18 ± 3, and 16 ± 1 μM of actinomycin-D, Hoechst 33258, and ethidium bromide, respectively, were required in order to achieve an equivalent level of inhibition in the presence of the RNA template. In fact, concentrations of at least 100 μM of the intercalator agents were required in order to be able to detect severe inhibition of the transcription from the RNA template. Similar levels of inhibition were also reported when actinomycin-D and ethidium bromide were added to the RNAP from *E. coli* acting on another RNA template (i.e., potato spindle tuber viroid) [10].

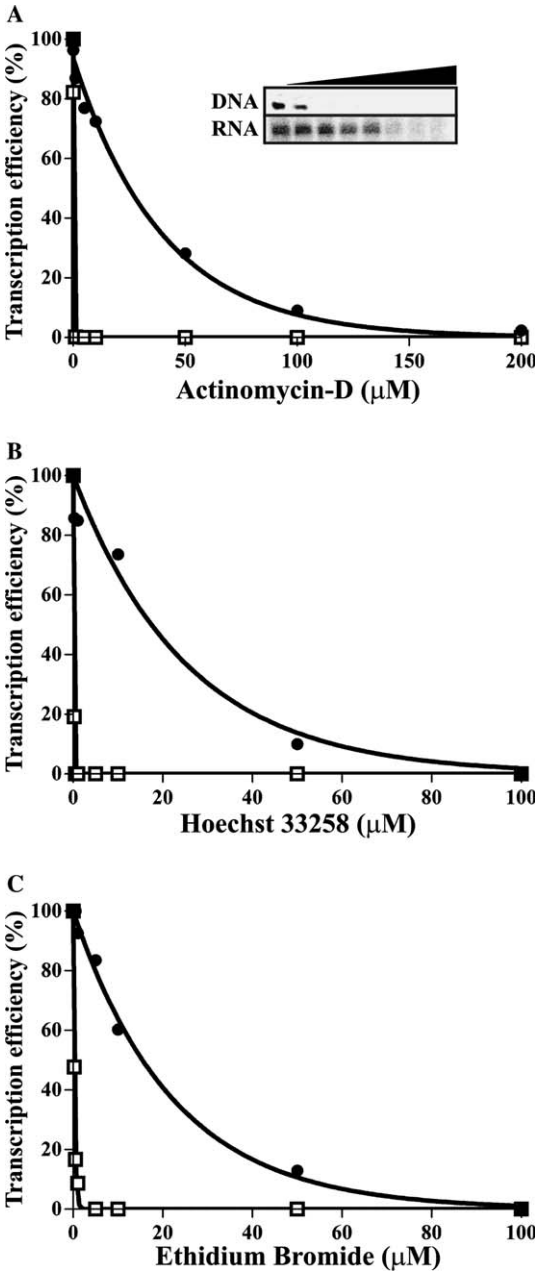

Fig. 2. Transcription sensitivity to various nucleic acid intercalators. The relative amounts of transcripts produced from either the P11.60 RNA (closed circles) or the DNA templates (open squares) are plotted as a function of the concentrations of intercalators (A–C). Typical gels showing the effect of increasing concentrations of actinomycin-D are presented in the inset of (A).

Ethidium bromide binding does not disrupt RNAP binding to P11.60

In order to establish that the intercalator agents inhibit transcription from the template by preventing the binding of *E. coli* RNAP, binding assays were performed in the presence of ethidium bromide. Either radioactive double-stranded DNA promoters or RNA promoter was preincubated in the transcription buffer containing increasing concentrations of ethidium bromide prior to the binding with the enzyme. Then the

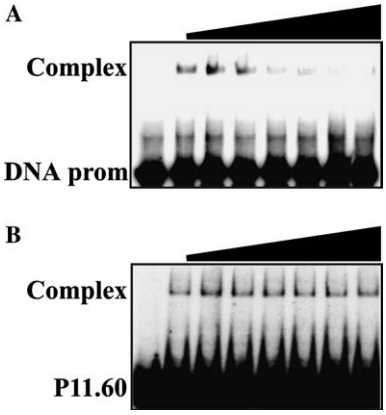

Fig. 3. Formation of RNAP:template complexes in the presence of ethidium bromide. Electrophoretic mobility-shift assay between the *E. coli* RNAP and either a double-stranded σ^{70}-driven DNA promoter (A) or the P11.60 RNA template (B) in the presence of increasing amounts of ethidium bromide (0, 0.5, 1, 5, 10, 50, and 100 μM). The first lane of both panels is a control reaction in which the RNAP was omitted.

resulting mixtures were analyzed by electrophoretic mobility-shift assay (Fig. 3A). Increasing the ethidium bromide concentration was observed to produce a smaller fraction of RNAP:DNA promoter complex. At concentrations high enough to completely inhibit the transcription reactions (i.e., 50 or 100 μM; see Fig. 2C), no RNAP:DNA promoter complex was detected. In contrast, the binding of the RNAP to the P11.60 RNA appeared to be unaffected by increasing concentrations of ethidium bromide (Fig. 3B).

The differences observed in the inhibitory effect may also reflect their differential intercalation efficiencies when acting on either the DNA or the RNA template. The degree of the intercalation of ethidium bromide was determined by monitoring its fluorescence spectrum. The optimal excitation and emission wavelengths for ethidium bromide were determined experimentally in the presence of the P11.60 RNA template. When excited at 335 nm, intercalated ethidium bromide fluorescence at 591 nm was greatly increased in the presence of either the DNA (Fig. 4, compared curves 1 versus 7) or the P11.60 RNA templates (Fig. 4, compared curves 4 versus 8). Consequently, the differences observed in the transcription inhibition caused by the intercalator agents most likely correspond to divergence in promoter binding by the polymerase, rather than differential binding of the compounds to either the DNA or the RNA template. This hypothesis receives additional support from the observation that the fluorescence spectrum of ethidium bromide was not decreased when P11.60 was preincubated with the RNAP prior to the addition of the intercalator. In fact, a slight increase of the fluorescence was repetitively observed in the presence of the polymerase, as compared to that seen with P11.60 alone (Fig. 4, compared curves 4 versus 3). If the

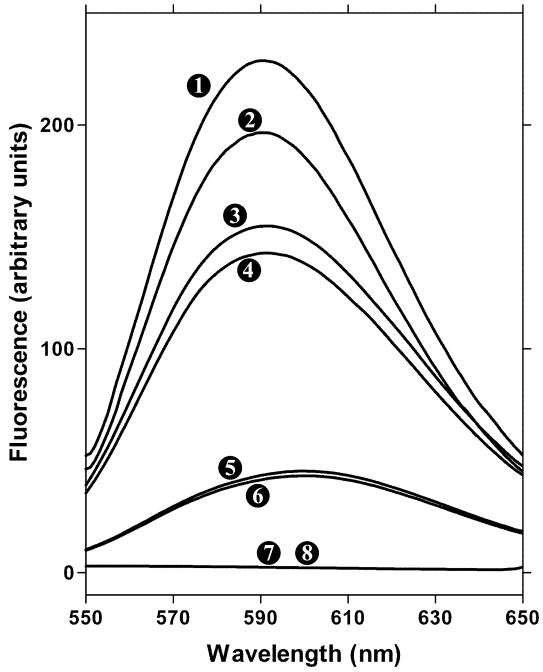

Fig. 4. Effect of the binding of *E. coli* RNAP to DNA and RNA promoters monitored by the fluorescence emission spectra of ethidium bromide (EtBr). (1) EtBr + DNA promoter; (2) EtBr + DNA promoter + RNAP; (3) EtBr + P11.60 + RNAP; (4) EtBr + P11.60; (5) EtBr + RNAP; (6) EtBr; (7) DNA promoter; and (8) P11.60. The background corrected fluorescence emission spectra were recorded at an excitation wavelength of 335 nm.

RNAP had bound to the double-stranded region of the RNA template, or if its binding required melting of the helical regions, the fluorescence signal should have been lowered, as it was observed in the case of the DNA template (Fig. 4, compared curves 1 versus 2). Thus, the difference in the mode of RNAP binding to the DNA and RNA templates might explain, at least in part, the differences in transcription levels observed in the presence of ethidium bromide. Moreover, these data lead to the suggestion that the RNAP binding site on the DNA promoter is in the double-stranded region, while that on the RNA promoter is in the single-stranded region (i.e., the loop of the P11.60 RNA, see Fig. 1B).

Binding site of, and region protected by, the RNAP

In order to confirm that the binding site of the RNAP is located in the single-stranded region (i.e., the loop of the P11.60 RNA), an oligonucleotide hybridization assay was performed. Internally labeled P11.60 RNA was preincubated either with or without the RNAP from *E. coli* prior to the addition of ribonuclease H (RNase H) and an excess of DNA oligonucleotides (9-mer) complementary to the P11.60 loop (Fig. 5A). The RNase H specifically cleaves DNA:RNA hybrids [11], therefore its use permits the monitoring of whether or not the oligonucleotides are bound to the RNA

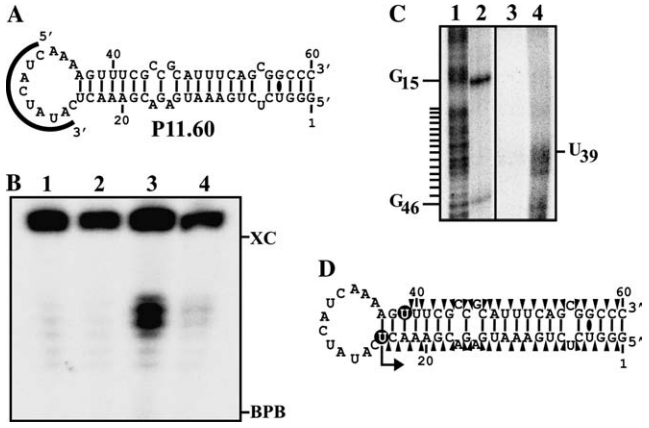

Fig. 5. Location of *E. coli* RNAP binding site. (A) Representation of the oligonucleotide hybridization assay including the P11.60 RNA and the position of the complementary oligonucleotide (bold line). (B) Protection by *E. coli* RNAP of the P11.60 loop from RNase H hydrolysis. Lane 1 contains the P11.60 RNA alone; lane 2 contains the P11.60 RNA in the presence of the RNase H, but in the absence of any oligonucleotides; lane 3 contains the P11.60 RNA incubated with both the RNase H and the oligonucleotides; and lane 4 is similar to the lane 3, but with prior incubation with the RNAP from *E. coli*. The positions of the xylene cyanol (XC) and the bromophenol blue (BPB) dyes are indicated adjacent to the gel. (C) Mapping of the binding site of *E. coli* RNAP on P11.60. End-labeled P11.60 RNAs were incubated with the RNAP from *E. coli* as described above and UV crosslinked. After precipitation, the RNAP:P11.60 template complexes were either reserved (lane 3) or submitted to partial alkaline hydrolysis (lane 4). Labeled P11.60 RNAs were also submitted to partial alkaline hydrolysis (lane 1) and RNase T1 digestion (lane 2) in order to provide molecular markers. The locations of the RNase T1 major cuts and the partial alkaline hydrolysis cleavage sites are indicated on the left of the gel. (D) Identification of the binding site of the RNAP on the P11.60 RNA template. The nucleotides crosslinked with the enzyme are circled, and the partial alkaline hydrolysis sites are indicated by arrows.

template. After the incubations, the mixtures were fractionated on a denaturing PAGE gel (Fig. 5B). No cleavage of the P11.60 RNA was detected in the absence of either RNase H or the oligonucleotides (Fig. 5B, lanes 1 and 2). In contrast, the addition of both the oligonucleotides and RNase H to the P11.60 RNA allowed detection of cleavage products of the appropriate size (i.e., ~30% cleavage; Fig. 5B, lane 3). Finally, when RNAP was preincubated with the P11.60 RNA, thereby allowing formation of the RNAP:P11.60 RNA complex, prior to the addition of RNase H and the DNA oligonucleotides, the amount of cleaved P11.60 RNA decreased significantly (i.e., <5% cleavage; Fig. 5B, lane 4). Moreover, it was shown that the binding of the polymerase to the oligonucleotide was marginal under the conditions tested (data not shown), therefore the observed decrease in cleavage in the presence of the RNAP was not caused by a titration of the oligonucleotides, even with a 10-fold excess of the oligonucleotides over the enzyme. It was also shown that the presence of RNAP did not affect the RNAse H hydrolysis when using another oligonucleotide/RNA target system that does not permit binding of the polymerase. Therefore, this result indicates that the RNAP from *E. coli* bound the large terminal loop and protected it from RNase H hydrolysis.

Further indication of the binding of the polymerase to the loop of the P11.60 RNA template came from footprinting analysis of crosslinked RNAP:P11.60 RNA complexes. Photoreactive 4-thio-uridines were incorporated into the P11.60 RNA during its in vitro synthesis in order to obtain a better crosslinking yield. The incorporation of 4-thio-uridine into the P11.60 RNA template affected neither the binding of the RNAP nor the transcription efficiency (data not shown). Briefly, 4-thio-uridine containing P11.60 RNA templates were end-labeled at either the 5′- or 3′-end using [γ-^{32}P]ATP and T4 polynucleotide kinase or [α-^{32}P]pCp and T4 RNA ligase, respectively, and purified through denaturing PAGE gels. These ^{32}P-labeled templates were incubated in the presence of RNAP prior to UV irradiation at 365 nm. The resulting mixtures were fractionated on a denaturing PAGE gel, the covalently linked RNAP:P11.60 RNA complexes were recovered and then submitted to a partial alkaline hydrolysis. A typical gel of an experiment performed using the 3′-end ^{32}P-labeled P11.60 RNA is illustrated in Fig. 5C. Partial hydrolysis of P11.60 RNA alone produced a ladder of bands corresponding to each position of the RNA backbone, while RNase T1 cuts specifically after the guanosine residues. The partial hydrolysis of the RNAP:P11.60 RNA complexes produced a ladder of bands corresponding to hydrolysis of the phosphodiester backbone between the 3′-end and U_{39}, which is the foremost 3′ thio-uridine crosslinked to the RNAP. The hydrolysis of the phosphodiester bonds located on the other side of the polymerase gave rise to products with a very slow electrophoretic mobility because of their covalent linkage with the RNAP. Similarly, the experiments performed with the 5′-end ^{32}P-labeled P11.60 RNA show that the region from G_1 to U_{24} was hydrolyzed. Since no uridine residues are located between U_{13} and U_{24}, the possibility that additional nucleotides are bound by the RNAP immediately upstream U_{24} cannot be excluded. However, the presence of RNAP was shown not to affect RNAse T1 hydrolysis of G_{14}, G_{16}, and G_{19} (data not shown). Taken together, our data indicate that the RNAP binds a region that includes the loop in its entirety and some of the adjacent nucleotides that are located within the stem (Fig. 5D).

Interaction of the β/β' subunits with P11.60

To find which RNAP subunits form close contact with the RNA template, the RNAP:P11.60 RNA complex was crosslinked and analyzed for protein content. Briefly, either the σ^{70}-driven DNA template or 4-thio-uridine containing P11.60 RNA was end-labeled at the 5′-end using [γ-^{32}P]ATP and T4 polynucleotide kinase.

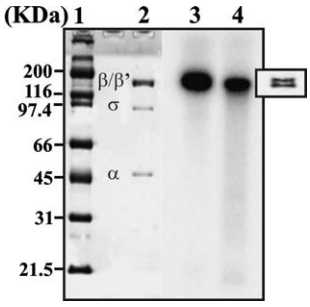

Fig. 6. Identification of the subunits of the RNAP included in the crosslinked complexes. Either end-labeled P11.60 RNA or the σ^{70}-driven DNA template was crosslinked with *E. coli* RNAP. Protein markers (lane 1) and the RNAP from *E. coli* (lane 2) were visualized by Coomassie blue staining. Lanes 3 and 4 are the experiments performed with the typical σ^{70}-driven DNA template and the P11.60 RNA template, respectively. The result of a longer migration of the RNAP:RNA complexes is shown in the inset.

Following purification through denaturing PAGE gels, these ^{32}P-labeled templates were incubated in the presence of RNAP. The complexes were then UV irradiated at 365 nm, fractionated on a denaturing PAGE gel, and visualized by autoradiography (Fig. 6). The non-crosslinked templates passed through the gel and therefore were not detected. Only the subunit(s) crosslinked to the templates were radioactive and therefore were detected. The migration of the subunits was not significantly affected by the presence of the templates because they are so small. A sample of RNAP was also migrated and stained with Coomassie blue in order to permit identification of the subunits. Only one band with an electrophoretic mobility corresponding to the β′/β subunits of the RNAP from *E. coli* was initially detected in the presence of either the DNA or the RNA templates. Extended electrophoresis revealed two bands corresponding to the β and β′ subunits of the RNAP (see inset Fig. 6). Whereas these results do not exclude the possibility that other RNAP subunits bind these two promoters, they are nevertheless in agreement with the involvement of the β and β′ subunits suggested by the severe inhibition of the polymerase activity on both templates caused by rifampicin (data not shown).

Discussion

We recently reported that an RNA hairpin structure can trigger the *E. coli* RNAP to initiate specific transcription [4]. With the exception of base-paired uridine as the primary initiation site, no specific sequence in both the stem and the loop was required as long as the RNA promoter adopts a rod-like conformation and a loop of at least 6 nt. The work reported here unambiguously demonstrates that the RNAP binding to the P11.60 template is primarily within the single-stranded hairpin loop. In the nature, the P11 loop of the peach latent mosaic viroid is composed by 12 nt in single-stranded region [13]. The RNAP-binding site explains the necessity to maintain a large terminal loop at this position of the RNA promoter. Most likely adoption of the stem by the template is strictly required to form this single-stranded RNA segment. However, if the same loop (or modified versions) are located between two double-stranded regions, the binding of the RNAP does not lead to a productive complex (data not shown).

We also found that both β and β′ subunits make close contacts within the loop of the RNA promoter. Since the bacterial RNAP structure shows that the catalytic center of the enzyme is intimately constructed from elements of both β and β′ subunits, our result suggests a similar mechanism between both DNA and RNA-directed transcription. The finding that *E. coli* RNAP forms also close contacts between the catalytic β′/β subunits and a DNA promoter agrees with this hypothesis [9]. Additionally, when single-stranded, the −10 region of DNA promoters is reported to contribute to the stabilization of the RNAP:DNA promoter complex [12]. The binding of the enzyme to the single-stranded domain of the P11.60 RNA template most likely reflects a similar mechanism, and also might explain the non-involvement of the σ^{70} subunit in promoter binding and melting [4].

In summary, this study presents an original description of the recognition of an RNA promoter by a DNA-dependent RNAP. Transcription from such a RNA template by the DNA-dependent RNAP from *E. coli* is obviously a non-physiological reaction. However, it is interesting to note that in the proposed secondary structure of PLMVd, the loop implicated in the replication initiation is located at the end of a long external stem [13,14]. For the potato spindle tuber viroid, a large external loop was also reported to be capable of binding the wheat germ DNA-dependent RNAP II [15]. RNA segments containing large external loops were also reported to initiate RNA synthesis from avocado sunblotch viroid and hepatitis *delta* virus RNAs [16–18]. Consequently, it is tempting to suggest that external hairpin structures may serve as RNA promoters for the replication of viroids and viroid-like satellite RNAs by host encoded DNA-dependent RNAPs. Likewise, it is not excluded to find reminiscent structures in cellular RNAs, which therefore, would have the potential for initiation of transcription from RNA templates rather than conventional DNA; whereas, physical evidences remain to be presented. If such a mechanism exists, it would modify significantly our understanding of the molecular biology of the cell.

Acknowledgments

This work was supported by a grant from the Natural Sciences and Engineering Research Council (NSERC) of Canada to J.P.P. M.P. was

the recipient of a post-doctoral fellowship from the Canadian Institutes of Health Research (CIHR). J.P.P. is an Investigator of the CIHR.

References

[1] A. Wettich, C.K. Biebricher, RNA species that replicate with DNA-dependent RNA polymerase from *Escherichia coli*, Biochemistry 40 (2001) 3308–3315.
[2] T.O. Diener, The viroid: biological oddity or evolutionary fossil?, Adv. Virus Res. 57 (2001) 137–184.
[3] M. Pelchat, F. Côté, J.P. Perreault, Study of the polymerization step of the rolling circle replication of peach latent mosaic viroid, Arch. Virol. 146 (2001) 1753–1763.
[4] M. Pelchat, C. Grenier, J.P. Perreault, Characterization of a viroid-derived RNA promoter for the DNA-dependent RNA polymerase from *Escherichia coli*, Biochemistry 41 (2002) 6561–6571.
[5] P.L. deHaseth, M.L. Zupancic, M.T. Record Jr., RNA polymerase-promoter interactions: the comings and goings of RNA polymerase, J. Bacteriol. 180 (1998) 3019–3025.
[6] S. Aktipis, N. Panayotatos, A kinetic study on the mechanism of inhibition of RNA synthesis catalyzed by DNA-dependent RNA polymerase. Differences in inhibition by ethidium bromide, 3,8-diamino-6-ethylphenanthridinium bromide and actinomycin D, Biochim. Biophys. Acta 655 (1981) 278–290.
[7] J. Ren, J.B. Chaires, Sequence and structural selectivity of nucleic acid binding ligands, Biochemistry 38 (1999) 16067–16075.
[8] G. Dougherty, The unwinding of circular DNA by intercalating agents as determined by gel electrophoresis, Biosci. Rep. 3 (1983) 453–460.
[9] V. Studitsky, K. Brodolin, Y. Liu, A. Mirzabekov, Topography of lac UV5 initiation complexes, Nucleic Acids Res. 29 (2001) 854–861.
[10] W. Rohde, H.R. Rackwitz, F. Boege, H.L. Sanger, Viroid RNA is accepted as a template for in vitro transcription by DNA-dependent DNA polymerase I and RNA polymerase from *Escherichia coli*, Biosci. Rep. 2 (1982) 929–939.
[11] H.H. Hogrefe, R.I. Hogrefe, R.Y. Walder, J.A. Walder, Kinetic analysis of *Escherichia coli* RNase H using DNA-RNA-DNA/DNA substrates, J. Biol. Chem. 265 (1990) 5561–5566.
[12] M.S. Fenton, J.D. Gralla, Function of the bacterial TATAAT −10 element as single-stranded DNA during RNA polymerase isomerization, Proc. Natl. Acad. Sci. USA 98 (2001) 9020–9025.
[13] M. Pelchat, D. Lévesque, J. Ouellet, S. Laurendeau, S. Lévesques, J. Lehoux, D.A. Thompson, K.C. Eastwell, L.J. Skrzeczkowski, J.P. Perreault, Sequencing of peach latent mosaic viroid variants from nine North American peach cultivars shows that this RNA folds into a complex secondary structure, Virology 271 (2000) 37–45.
[14] F. Bussière, J. Ouellet, F. Côté, D. Lévesque, J.P. Perreault, Mapping in solution shows the peach latent mosaic viroid to possess a new pseudoknot in a complex, branched secondary structure, J. Virol. 74 (2000) 2647–2654.
[15] T.C. Goodman, L. Nagel, W. Rappold, G. Klotz, D. Riesner, Viroid replication: equilibrium association constant and comparative activity measurements for the viroid-polymerase interaction, Nucleic Acids Res. 12 (1984) 6231–6246.
[16] J.A. Navarro, R. Flores, Characterization of the initiation sites of both polarity strands of a viroid RNA reveals a motif conserved in sequence and structure, EMBO J. 19 (2000) 2662–2670.
[17] M.R. Beard, T.B. Macnaughton, E.J. Gowans, Identification and characterization of a hepatitis delta virus RNA transcriptional promoter, J. Virol. 70 (1996) 4986–4995.
[18] J. Filipovska, M.M. Konarska, Specific HDV RNA-templated transcription by pol II in vitro, RNA 6 (2000) 41–54.